ELSEVIER

www.elsevier.nl/locate/jorganchem

Journal of Organometallic Chemistry 601 (2000) 271–283

Journal of Organometallic Chemistry

Regiospecificity in reactions of alkynes and phosphines with the phosphido-bridged iron–cobalt complex $[(OC)_4Fe(\mu\text{-}PPh_2)Co(CO)_3]$

Jason D. King [a,1], Martin J. Mays* [a,2], Chi-Yu Mo [a], Paul R. Raithby [a], Moira A. Rennie [a], Gregory A. Solan* [b,3], Trushar Adatia [c], Gráinne Conole [c]

[a] *Department of Chemistry, Lensfield Road, Cambridge CB2 1EW, UK*
[b] *Department of Chemistry, University of Leicester, University Road, Leicester LE1 7RH, UK*
[c] *School of Applied Chemistry, University of North London, Holloway Road, London N7 8DB, UK*

Received 22 November 1999; accepted 18 January 2000

Abstract

The iron–cobalt phosphido-bridged complex $[(OC)_4Fe(\mu\text{-}PPh_2)Co(CO)_3]$ (**1**) can be prepared conveniently and in good yield from the reaction of $[Co_2(\mu\text{-}PPh_2)_2(CO)_6]$ with $[Fe(CO)_5]$. A study of the reactivity of **1** towards symmetrical and unsymmetrical alkynes, $R^1C{\equiv}CR^2$ ($R^1 = R^2 = CO_2Me$, Ph; $R^1 = H$, $R^2 = Ph$), has been undertaken. In all cases, five-membered ferracycle-containing products of the type $[(OC)_3Fe\{\mu\text{-}PPh_2C(O)CR^1CR^2\}Co(CO)_3]$ ($R^1 = R^2 = CO_2Me$ (**2a**), Ph (**2c**); $R^1 = H$, $R^2 = Ph$ (**2b**)), are initially obtained in which a molecule of CO and a molecule of $R^1C{\equiv}CR^2$ have been inserted regiospecifically into a Co–P bond in **1**. Decarbonylation of **2a** occurs during its preparation or in low yield on its thermolysis to give the four-membered ferracyclic species $[(OC)_3Fe\{\mu\text{-}PPh_2C(CO_2Me)C(CO_2Me)\}Co(CO)_3]$ (**3a**). Similar thermolysis of **2b** results not only in the related decarbonylation product $[(OC)_3Fe(\mu\text{-}PPh_2CHCPh)Co(CO)_3]$ (**3b**), but additionally in three other products all in low yield, namely the regioisomer of **3b**, $[(OC)_3Fe(\mu\text{-}PPh_2CPhCH)Co(CO)_3]$ (**4b**), the aldehyde-substituted complex $[(OC)_3Fe\{\mu\text{-}PPh_2C(CHO)CPh\}Co(CO)_3]$ (**5b**) and the five-membered ferracycle-containing species $[(OC)_3Fe\{\mu\text{-}PPh_2CHCPhC(O)\}Co(CO)_3]$ (**6b**). Treatment of **2a** and **2b** with $PPhMe_2$ and $P(OMe)_3$ results in substitution of an iron-bound carbonyl group to give, respectively, $[(PhMe_2P)(OC)_2Fe\{\mu\text{-}PPh_2C(O)C(CO_2Me)C(CO_2Me)\}(\mu\text{-}CO)Co(CO)_2]$ (**7a**) and $[\{(MeO)_3P\}(OC)_2Fe\{\mu\text{-}PPh_2C(O)CHCPh\}(\mu\text{-}CO)Co(CO)_2]$ (**7b**) in high yield. In contrast, substitution of a cobalt-bound carbonyl is achieved on reaction of **3a** with $PPhMe_2$ or PPh_2H to give $[(OC)_3Fe\{\mu\text{-}PPh_2C(CO_2Me)C(CO_2Me)\}Co(CO)_2(L)]$ ($L = PPhMe_2$ (**8a**), PPh_2H (**9a**)). Thermolysis of the secondary phosphine-substituted complex **9a** results in phosphorus–hydrogen bond cleavage to give $[(OC)_3Fe\{\mu\text{-}PPh_2C(CO_2Me)CH(CO_2Me)\}(\mu\text{-}PPh_2)Co(CO)_2]$ (**10a**). Single-crystal X-ray diffraction studies have been performed on complexes **7b**, **8a** and **10a**.

Keywords: Cobalt; Iron; Phosphido; Alkyne; Dinuclear; Phosphine

1. Introduction

The chemistry of bimetallic transition-metal carbonyl complexes tethered together by phosphido groups ($\mu\text{-}PR_2$) (R = hydrocarbyl) has been the focus of a large number of reports. Originally, it was envisaged that the bridging phosphido group could behave as an inert spectator ligand capable of supporting a polynuclear framework during a range of catalytic processes [1]. However, there are now many reports in which the phosphido group can participate in a transformation, particularly in homobimetallic iron [2] and cobalt chemistry [3]. For example, the reaction of an alkyne with the diiron phosphido-/acetylido-bridged complex $[(OC)_3Fe\{\mu\text{-}CC(CMe_3)\}(\mu\text{-}PPh_2)Fe(CO)_3]$ leads to coupling of the alkyne, acetylide, a carbonyl and the phosphido group to give $[(OC)_3Fe\{\mu\text{-}CRCRCC(CMe_3)C(O)PPh_2\}Fe(CO)_2]$ [2a]. Contrastingly, the reaction of alkyne with the dicobalt bis-phosphido-bridged species $[(OC)_3Co(\mu\text{-}PPh_2)_2Co(CO)_3]$ leads to coupling of two molecules of alkyne, carbonyl and

[1] Present address: Department of Chemistry, The University of Montana, Missoula, MT 59812, USA.
[2] *Corresponding author. Fax: +44-1223-336362; e-mail: mjm14@cam.ac.uk
[3] *Corresponding author.

0022-328X/00/$ - see front matter
PII: S0022-328X(00)00082-6

both phosphido groups to give $[(OC)_2Co\{\mu\text{-}PPh_2CRCRC(O)CRCRPPh_2\}Co(CO)_2]$ [3a].

Given the diverse chemistry that occurs for both the diiron and dicobalt phosphido-bridged homobimetallic complexes, we decided to examine the chemistry of a heterobimetallic Fe–Co phosphido-bridged system. In this paper we have been concerned with the synthesis and reactions of the Group 8–Group 9 phosphido-bridged complex $[(OC)_4Fe(\mu\text{-}PPh_2)Co(CO)_3]$ (**1**) with symmetrical and unsymmetrical alkynes. In addition, the reactivity of number of the resulting products towards secondary and tertiary phosphines has been examined.

2. Results and discussion

2.1. Preparation of $[(OC)_4Fe(\mu\text{-}PPh_2)Co(CO)_3]$ (1)

The complex $[(OC)_4Fe(\mu\text{-}PPh_2)Co(CO)_3]$ (**1**) has previously been synthesised by two different routes. Thompson and co-workers originally prepared it from the reaction of $[Fe(CO)_4(PPh_2H)]$ with $[(\eta^3\text{-}C_3H_5)Co(CO)_3]$ [4] while Schmid and co-workers isolated it in low yield by adding $[Fe_2(CO)_9]$ to a reaction mixture of $Na[Co(CO)_4]$ and PPh_2Cl [5]. In view of the accessibility of $[Co_2(\mu\text{-}PPh_2)_2(CO)_6]$ and its demonstrated ability to act as a source of $[(OC)_4CoPPh_2]$ [6], we have prepared **1** in high yield from the reaction of $[Co_2(\mu\text{-}PPh_2)_2(CO)_6]$ with $[Fe(CO)_5]$ in toluene at 353 K (Eq. (1)).

(1)

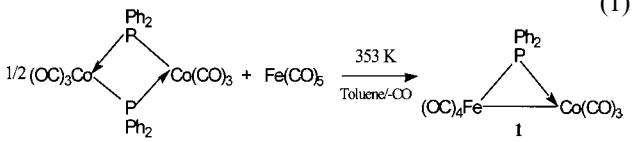

The complex prepared in this way was found to show the same spectroscopic properties as when it was originally prepared by the routes discussed above [4,5].

2.2. Reactions of $[(OC)_4Fe(\mu\text{-}PPh_2)Co(CO)_3]$ (1) with $R^1C{\equiv}CR^2$

The reaction of **1** with an equimolar amount of $R^1C{\equiv}CR^2$ ($R^1 = R^2 = CO_2Me$, Ph; $R^1 = H$, $R^2 = Ph$) was found to occur readily in THF at 318 K (Scheme 1). The optimum reaction time was found to vary according to the alkyne employed. For $R^1 = R^2 = CO_2Me$, two products $[(OC)_3Fe\{\mu\text{-}PPh_2C(O)C(CO_2Me)C(CO_2Me)\}Co(CO)_3]$ (**2a**) and $[(OC)_3Fe\{\mu\text{-}PPh_2C(CO_2Me)C(CO_2Me)\}Co(CO)_3]$ (**3a**) were formed in approximately equal yield. With $R^1 = H$, $R^2 = Ph$ and $R^1 = R^2 = Ph$, however, only one product, $[(OC)_3Fe\{\mu\text{-}PPh_2C(O)CHCPh\}Co(CO)_3]$ (**2b**) or $[(OC)_3Fe\{\mu\text{-}PPh_2C(O)CPhCPh\}Co(CO)_3]$ (**2c**), was observed to form in appreciable yield. All the complexes have been characterised by mass spectrometry, microanalysis and by ^{1}H-, ^{31}P-, ^{13}C-NMR and IR spectroscopy (see Table 1 and Section 3).

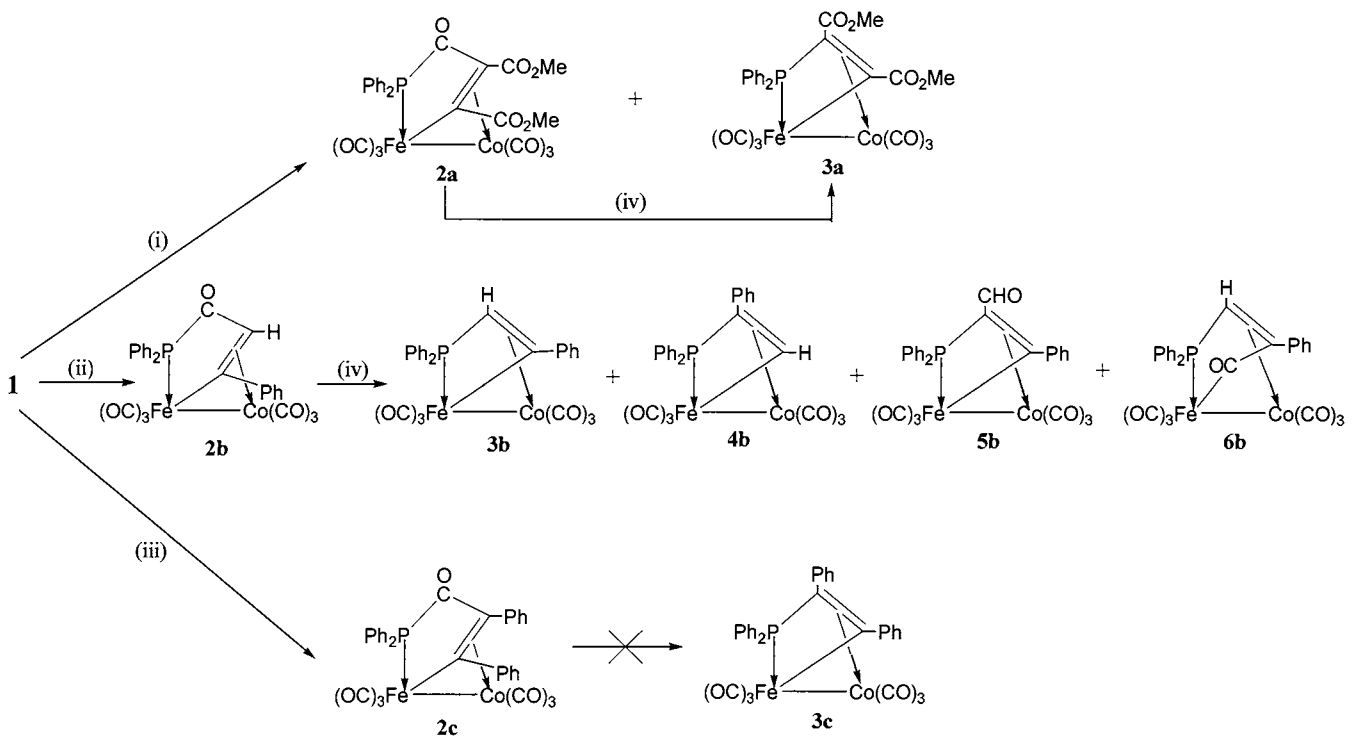

Scheme 1. Products from the reactions of $[(OC)_4Fe(\mu\text{-}PPh_2)Co(CO)_3]$ (**1**) with $R^1C{\equiv}CR^2$; (i) $C_2(CO_2Me)_2$, 313 K, THF, 3 h; (ii) PhCCH, 318 K, THF, 1.5 h; (iii) PhCCPh, 323 K, THF, 16 h; (iv) 333 K, THF, 18 h.

Table 1
IR, ^{1}H- and ^{31}P-NMR data for the new complexes **2–10**

Compound	ν(CO) (cm^{-1}) [a]	^{1}H-NMR (δ) [c]	^{31}P-NMR (δ) [d]
2a	2090m, 2060vs, 2033s, 2012m, 1936w, 1731w	7.9–7.2[m, 10H, Ph], 3.87[s, 3H, CO_2Me], 3.82[s, 3H, CO_2Me]	−79.2[s, Fe–PPh$_2$C(O)C(CO_2Me)C(CO_2Me)]
2b	2074m, 2045vs, 2016s, 1998s, 1932w, 1740w, 1632w	7.9–7.2[m, 15H, Ph], 5.25[d, ^{3}J(PH) 39, 1H, PPh$_2$C(O)CHCPh]	−81.6[s, Fe–PPh$_2$C(O)CHCPh]
2c	2064m, 2030vs, 2001s, 1989m, 1970w	7.9–7.3[m, 20H, Ph]	−153.3[s, Fe–PPh$_2$C(O)CPhCPh]
3a	2082s, 2046s, 2024s, 1998m, 1984m, 1712m	7.9–7.3[m, 10H, Ph], 3.84[s, 3H, CO_2Me], 3.63[s, 3H, CO_2Me]	−148.0[s, Fe–PPh$_2$C(CO_2Me)C(CO_2Me)]
3b	2067s, 2029vs, 2004s, 1992sh, 1974m, 1943w	8.0–7.0[m, 15H, Ph], 4.84[d, ^{2}J(PH) 4.8, PPh$_2$CHCPh]	−158.1[s, Fe–PPh$_2$CHCPh]
4b	2068s, 2029s, 2004s, 1992s, 1973sh, 1944w	8.2–7.0[m, 15H, Ph], 4.96[d, ^{3}J(PH) 33.6, PPh$_2$CPhCH]	−149.1[s, Fe–PPh$_2$CPhCH]
5b	2076s, 2043s, 2016s, 2001s, 1982sh, 1971w, 1938m, 1636m	8.95[d, ^{3}J(PH) 1.4, 1H, CHO], 8.0–7.1[m, 15H, Ph]	−84.6[s, Fe–PPh$_2$C(CHO)CPh]
6b	2078m, 2045vs, 2029m, 2020m, 1999w, 1988w, 1629w	8.1–7.2[m, 15H, Ph], 4.78[d, ^{2}J(PH) 0.74, 1H, PPh$_2$CHCPhC(O)]	−83.2[s, Fe–PPh$_2$CHCPhC(O)]
7a	2053m, 2021s, 2008sh, 1977m, 1859w, 1722sh, 1713w, 1617w [b]	8.0–7.1[m, 15H, Ph], 3.78[s, 3H, CO_2Me], 3.70[s, 3H, CO_2Me], 1.89[d, ^{2}J(PH) 9.8, 3H, PPhMe_2], 1.77[d, ^{2}J(PH) 9.3, 3H, PPhMe_2]	−80.1[d, ^{2}J(PP) 123, Fe–PPh$_2$C(O)C(CO_2Me)C(CO_2Me)], −132.9[d, Fe–PPhMe$_2$]
7b	2043m, 2011s, 1988m, 1966m, 1890w [b]	8.1–7.1[m, 15H, Ph], 5.31[d, ^{3}J(PH) 39.9, 1H, PPh$_2$C(O)CHCPh], 3.07[d, ^{3}J(PH) 11.0, 9H, P(OMe)$_3$]	16.9[d, ^{2}J(PP) 69, Fe–P(OMe)$_3$], −87.9[d, Fe–PPh$_2$C(O)CHCPh]
8a	2049vs, 1997s, 1987sh, 1964m, 1699w, 1687wsh [b]	7.9–7.2[m, 15H, Ph], 3.91[s, 3H, CO_2Me], 2.79[s, 3H, CO_2Me], 1.72[d, ^{2}J(PH) 10.0, 3H, PPhMe_2], 1.59[d, ^{2}J(PH) 8.8, 3H, PPhMe_2]	−118.0[s, br, Co–PPhMe$_2$], −144.8[d, ^{3}J(PP) 15, Fe–PPh$_2$C(CO_2Me)C(CO_2Me)]
9a	2054s, 2006s, 1992s, 1972m, 1894w [b]	8.2–7.0[m, 20H, Ph], 6.02[d, ^{1}J(PH) 366.0, 1H, PPh$_2H$], 3.91[s, 3H, CO_2Me], 2.88[s, 3H, CO_2Me]	−108.0[d, ^{3}J(PP) 9, Co–PPh$_2$H], −146.1[d, ^{3}J(PP) 9, Fe–PPh$_2$C(CO_2Me)C(CO_2Me)]
10a	2051s, 2026vs, 1997m, 1988s, 1964s, 1718w, 1558w, 1540w	8.0–6.7[m, 20H, Ph], 4.02[dd, ^{3}J(PH) 21.6, ^{3}J(P′H) 3.2, 1H, PPh$_2$C(CO_2Me)CH(CO_2Me)], 3.81[s, 3H, CO_2Me], 3.68[s, 3H, CO_2Me]	31.7[s, br, μ-PPh$_2$], −89.7[d, ^{2}J(PP) 38, Fe–PPh$_2$C(CO_2Me)CH(CO_2Me)]

[a] Recorded in *n*-hexane solution.
[b] Recorded in CH_2Cl_2 solution.
[c] ^{1}H chemical shifts (δ) in ppm relative to $SiMe_4$ (0.0 ppm), coupling constants in Hz in $CDCl_3$ at 293 K.
[d] ^{31}P chemical shifts (δ) in ppm relative to external P(OMe)$_3$ (0.0 ppm) (upfield shifts negative). Add 140.2 to tabulated values in order to reference relative to external 85% H_3PO_4. Spectra were {^{1}H}-gated decoupled and measured in $CDCl_3$ at 293 K.

The spectroscopic properties of **2** are consistent with the structures depicted in Scheme 1. The IR spectra each show absorptions in the terminal carbonyl region and peaks in the range 1600–1700 cm^{-1} corresponding to the inserted carbonyl groups, while the fast atom bombardment (FAB) mass spectra display molecular ions and fragmentation peaks corresponding to loss of up to five carbonyl groups. The ^{1}H-NMR spectra of **2** show, in addition to phenyl resonances, two methyl signals for **2a** and a doublet resonance (^{3}J(PH) 39.2 Hz) at δ 5.25 for the CH proton of the metallacycle in **2b**. The sharpness of the single signal in the ^{31}P-NMR spectra of **2** indicates that the phosphide group of the metallacycle is bound to iron (rather than to the quadrupolar ^{59}Co).

The pathway by which the insertion of an alkyne and a CO molecule into a metal–phosphorus bond in **1** occurs to give **2** is uncertain, but is believed to proceed by a similar route to that postulated for the closely related reactions of [(OC)$_4$Ru(μ-PPh$_2$)Co(CO)$_3$] with alkynes [7]. Scheme 2 shows a possible pathway involving association of the alkyne at the cobalt centre in **1** with metal–metal bond rupture followed by metal–metal bond closure and carbon–carbon bond coupling and finally reductive elimination (promoted by P–C bond coupling) to give **2**.

2.3. Thermolysis of complexes 2

The five-membered metallacyclic complexes **2a** and **2b** were found to undergo thermolytic decarbonylation (Scheme 1). When solutions of **2a** and **2b** were heated to 333 K in THF for 18 h, loss of CO from the five-membered ferracycle in both cases led to the four-membered ferracyclic complexes [(OC)$_3$Fe{μ-PPh$_2$C(CO_2Me)C(CO_2Me)}Co(CO)$_3$] (**3a**) and [(OC)$_3$Fe{μ-PPh$_2$-

CHCPh}Co(CO)$_3$] (**3b**) in low yields. In addition, the thermolysis of **2b** gave rise to three other products also in low yield; the regioisomer of **3b**, [(OC)$_3$Fe{μ-PPh$_2$CPhCH}Co(CO)$_3$] (**4b**), the aldehyde-substituted complex, [(OC)$_3$Fe{μ-PPh$_2$C(CHO)CPh}Co(CO)$_3$] (**5b**) and the five-membered ferracycle-containing species [(OC)$_3$Fe{μ-PPh$_2$CHCPhC(O)}Co(CO)$_3$] (**6b**). Complex **2c** was found to be stable to thermolysis under these conditions. Complexes **3**–**6** were characterised by mass spectrometry, microanalysis and by ^{1}H-, ^{31}P-, ^{13}C-NMR and IR spectroscopy (see Table 1 and Section 3).

The spectroscopic properties of **3**–**6** are consistent with the structures illustrated in Scheme 1. All the complexes display molecular ion peaks along with fragmentation peaks corresponding to the loss of carbonyl groups. In the IR spectra of **3**–**6**, in addition to terminal carbonyl absorptions, complexes **3a**, **5b** and **6b** display carbonyl bands at lower wavenumber corresponding, respectively, to CO_2Me groups (1712 cm^{-1}), a CHO group (1636 cm^{-1}) and an inserted CO group (1629 cm^{-1}).

^{1}H-NMR is particularly useful in assigning the regioisomers **3b** and **4b** with a doublet resonance being seen in both cases for the vinyl protons. In **3b** the doublet splitting of 4.8 Hz is due to a geminal coupling to phosphorus while in **4b** the three-bond *trans* coupling to phosphorus leads to a value for the coupling of 33.6 Hz [8]. Complex **5b** is most conveniently identified as possessing a free aldehyde group by its ^{1}H-NMR spectrum which contains a doublet (^3J(PH) 1.4 Hz) at δ 8.95 while in **6b** the lone vinylic proton can be seen at δ 4.78 with a geminal coupling of 0.74 Hz. As with complexes **2**, the ^{31}P-NMR spectra of **3**–**6** each possess a single sharp resonance corresponding to a phosphorus atom bound to iron.

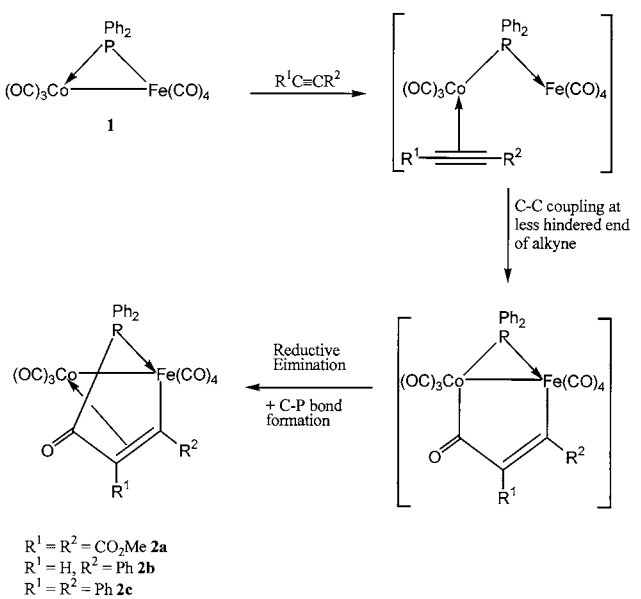

Scheme 2. Possible pathway to account for the formation of **2** from the reaction of **1** with R^{1}C≡CR^2.

Decarbonylation of a five-membered metallacycle to give a four-membered metallacycle has been previously observed during the thermolysis of [(OC)$_3$Ru{μ-PPh$_2$C(O)CR^{1}CR^2}Co(CO)$_3$] [7]. This current study of the thermolytic reactions of the ferracyclic family of complexes **2** shows a similar tendency (except for **2c**) for decarbonylation of the metallacycle. Notably in the case of **2b**, in which R^1 and R^2 are inequivalent, initial decarbonylation results in the formation of both the regioisomers (**3b** and **4b**). In contrast, decarbonylation of [(OC)$_3$Ru{μ-PPh$_2$C(O)CR^{1}CR^2}Co(CO)$_3$] (R^2 = Ph, Bu^t; R^1 = H) gives, in both cases, only one regioisomer [7]. The explanation for the lack of regiospecificity in the initial decarbonylation of **2b** to give **3b** and **4b** and the unexpected formation of **5b** and **6b** in the present work is uncertain. Scheme 3, however, shows possible pathways that can account for the formation of **3b**–**6b** from **2b**. Whether **3b** or **4b** is formed from intermediate **A** depends upon the Fe–C(alkyne) bond into which the PPh$_2$ fragment inserts. The formation of **5b** and **6b** from **2b** follows the recarbonylation of intermediate **A**.

2.4. Reactions of 2 and 3 with organo-phosphines or -phosphites

Both complexes **2** and **3** possess three carbonyl groups bound to each iron and cobalt centre but differ in the nature of the bridging ligand, viz. PPh$_2$CRCR versus PPh$_2$C(O)CRCR. It was of interest to determine the regioselectivity of carbonyl substitution by organophosphines or -phosphites in these related Fe–Co complexes. Scheme 4 shows the reactions of the **2a** and **2b** with PPhMe$_2$ and P(OMe)$_3$, respectively, and of **3a** with PPhMe$_2$ and PPh$_2$H.

Complex **2a** was observed to react rapidly with PPhMe$_2$ in toluene at 313 K to give the iron-bound PPhMe$_2$-substituted product [(MePh$_2$P)(OC)$_2$Fe{μ-PPh$_2$C(O)C(CO$_2$Me)C(CO$_2$Me)}(μ-CO)Co(CO)$_2$] (**7a**) in near quantitative yield. Similarly, complex **2b** reacts with P(OMe)$_3$ to give [{(MeO)$_3$P}(OC)$_2$Fe{μ-PPh$_2$C(O)C(CO$_2$Me)C(CO$_2$Me)}(μ-CO)Co(CO)$_2$] (**7b**). The reaction of **3a** in toluene with either PPhMe$_2$ or PPh$_2$H also gave simple mono-substitution products [(OC)$_3$Fe{μ - PPh$_2$C(O)C(CO$_2$Me)C(CO$_2$Me)}Co(CO)$_2$-(PPhMe$_2$)] (**8a**) and [(OC)$_3$Fe{μ-PPh$_2$C(O)C(CO$_2$Me)C-(CO$_2$Me)}Co(CO)$_2$(PPh$_2$H)] (**9a**) in high yield but notably with substitution of a cobalt- rather than iron-bound carbonyl group occurring in both cases. All the above complexes have been characterised by a combination of mass spectrometry, microanalysis and by IR, ^{1}H-, ^{13}C- and ^{31}P-NMR spectroscopy (see Table 1 and Section 3). In addition complexes **7b** and **8a** have been the subjects of single-crystal X-ray diffraction studies.

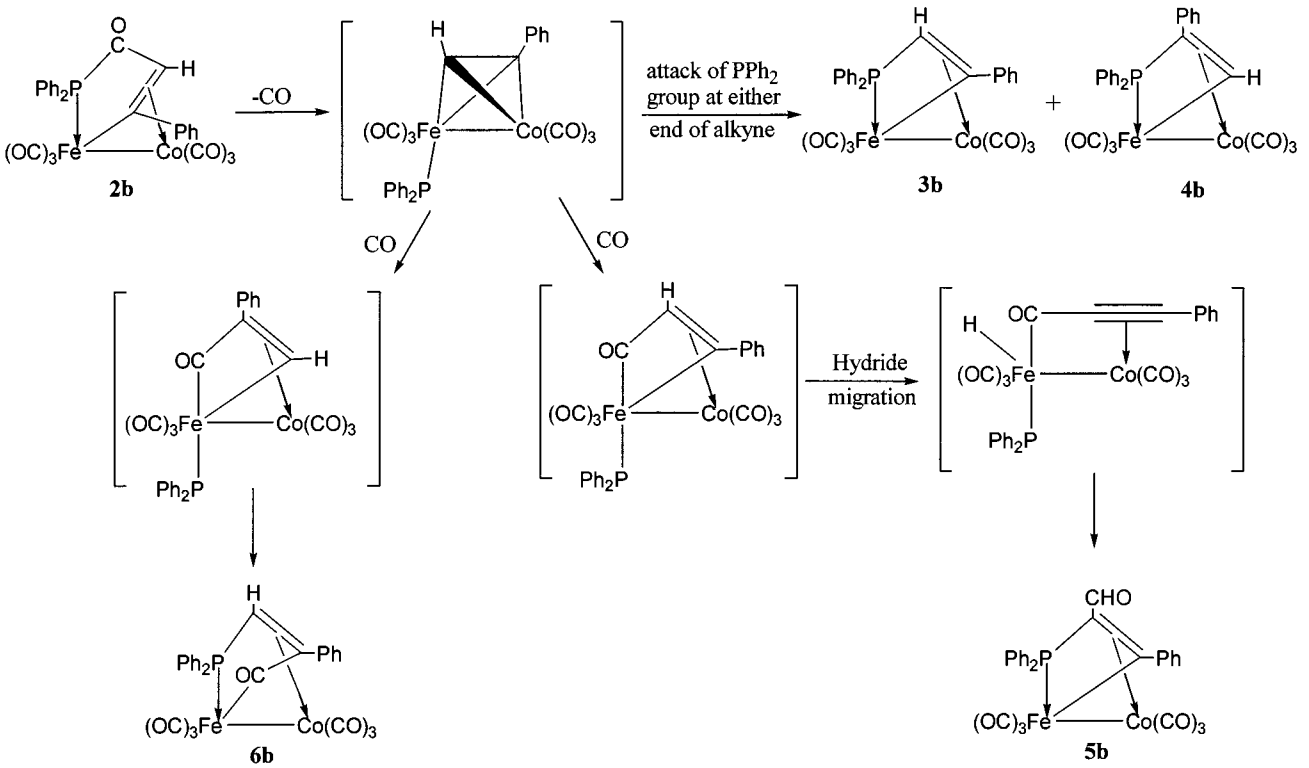

Scheme 3. Possible pathway to account for the formation of **3b**–**6b** from **2b**.

Suitable crystals of **7b** for an X-ray diffraction study were grown by diffusion of hexane into a dichloromethane solution of **7b**. The molecular structure is depicted in Fig. 1; selected bond lengths and angles are listed in Table 2. The structure of **7b** consists of a core of two metal atoms, cobalt and iron, which are singly bonded (Fe–Co 2.595(2) Å). The two metal atoms are also linked together by means of two bridging ligands. The first of these is a carbonyl group that bridges asymmetrically (Co–C(11) 1.73(1) vs. Fe–C(11) 2.40(1) Å) and the other consists of a five-membered metallacycle incorporating the iron atom. The metallacycle also incorporates a PPh_2 group, a carbonyl group and a phenylacetylene derived unit that is η^2-coordinated to cobalt. This two-carbon unit is regiospecifically oriented such that the terminus bonded to a phenyl group is also bonded directly to the iron atom whilst the terminus bonded to a hydrogen atom is bonded to the ring carbonyl group. The remaining ligands are two terminal carbonyl groups bound to cobalt and two carbonyl groups and a $P(OMe)_3$ group bound to the iron atom. The $P(OMe)_3$ ligand occupies a pseudo-axial site (P(2)–Fe(1)–Co(1) 141.7(1)°). The general structure is similar to that of the RuCo complex $[(OC)_3Ru\{\mu\text{-}PPh_2C(O)CPhCPh\}Co(CO)_3]$ [7] and to the Co_2 complex $[Co_2\{\mu\text{-}PPh_2C(O)CHCH\}(CO)_3(PPh_3)]$ [9].

It is interesting to note that the solid-state structure of **7b** contains a bridging carbonyl, which is also indicated in the IR spectrum of **7b** by an absorption band at 1890 cm^{-1}. This IR absorption band is also found in the related unsubstituted Ru–Co complex $[(OC)_3Ru\{\mu\text{-}PPh_2C(O)CPhCPh\}Co(CO)_3]$ (at 1900 cm^{-1}) [7]. However, the unsubstituted complexes **2** exhibit no such absorptions and have therefore been assigned structures with terminal carbonyl groups only. It is proposed that

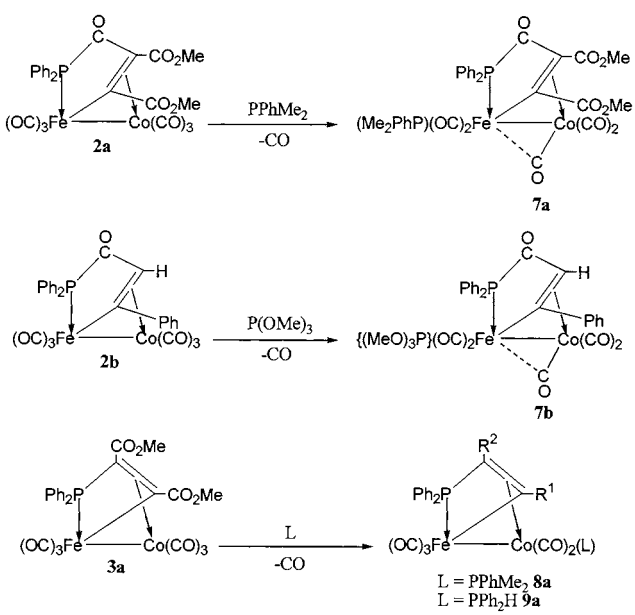

Scheme 4. Products from the reactions of **2** and **3** with organo-phosphines and -phosphites.

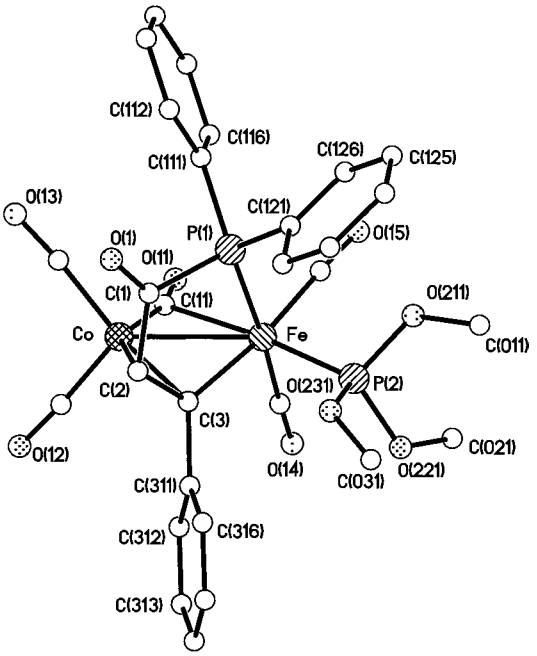

Fig. 1. Molecular structure of [{(MeO)$_3$P}(OC)$_2$Fe{μ-PPh$_2$C(O)CHCPh}(μ-CO)Co(CO)$_2$] (**7b**) including the atom numbering scheme.

Table 2
Selected bond lengths (Å) and angles (°) for [{(MeO)$_3$P}(OC)$_2$Fe{μ-PPh$_2$C(O)CHCPh}(μ-CO)Co(CO)$_2$] (**7b**)

Bond lengths			
Co–Fe	2.595(2)	Fe–P(1)	2.256(3)
Fe–P(2)	2.161(4)	Fe–C(3)	2.027(10)
Fe–C(11)	2.397(13)	Fe–C(14)	1.788(12)
Fe–C(15)	1.797(14)	Co–C(2)	2.140(11)
Co–C(3)	2.012(10)	Co–C(11)	1.730(13)
Co–C(12)	1.739(14)	Co–C(13)	1.779(13)
C(1)–O(1)	1.248(14)	C(1)–C(2)	1.475(15)
C(2)–C(3)	1.426(14)		
Bond angles			
C(2)–Co–Fe	78.8(3)	C(3)–Co–Fe	50.3(3)
C(13)–Co–Fe	127.6(5)	C(11)–Co–Fe	63.7(4)
C(12)–Co–Fe	127.9(4)	C(11)–Co–C(2)	142.3(5)
C(3)–Co–C(2)	40.0(4)	C(11)–Co–C(3)	109.2(5)
C(12)–Co–C(2)	104.7(5)	C(12)–Co–C(3)	99.6(5)
C(13)–Co–C(2)	99.4(5)	C(13)–Co–C(3)	137.7(5)
C(13)–Co–C(11)	100.0(6)	C(12)–Co–C(11)	101.8(6)
C(13)–Co–C(12)	103.6(6)	P(1)–Fe–Co	76.3(1)
P(2)–Fe–Co	141.7(1)	C(3)–Fe–Co	49.8(3)
C(11)–Fe–Co	40.3(3)	C(14)–Fe–Co	98.6(4)
P(2)–Fe–P(1)	94.2(1)	C(3)–Fe–P(1)	84.5(3)
C(3)–Fe–P(2)	92.9(3)	C(11)–Fe–P(1)	93.7(3)
C(11)–Fe–P(2)	172.1(3)	C(11)–Fe–C(3)	86.9(4)
C(14)–Fe–P(1)	174.2(4)	C(14)–Fe–P(2)	91.5(4)
C(14)–Fe–C(3)	94.3(5)	C(14)–Fe–C(11)	80.6(5)
C(15)–Fe–Co	124.0(4)	C(15)–Fe–P(1)	90.6(4)
C(15)–Fe–P(2)	92.6(4)	C(15)–Fe–C(3)	172.9(5)
C(15)–Fe–C(11)	88.2(5)	C(15)–Fe–C(14)	90.0(6)
C(1)–P(1)–Fe	102.3(4)	C(111)–P(1)–Fe	120.0(3)
C(111)–P(1)–C(1)	106.8(4)	C(121)–P(1)–Fe	121.4(3)
C(121)–P(1)–C(1)	103.4(4)	C(121)–P(1)–C(111)	101.2(4)

the difference arises as a result of the variation in electron density at the iron (or ruthenium) atom. In complex **7b**, the electron density at Fe is particularly high on account of P(OMe)$_3$ being a good σ-donor and poor π-acceptor, therefore the excess electron density is dispersed onto a bridging carbonyl group.

Suitable crystals of **8a** for an X-ray diffraction study were grown by diffusion of hexane into a dichloromethane solution of the complex. The molecular structure is shown in Fig. 2; selected bond lengths and angles are given in Table 3.

The structure consists of cobalt and iron atoms bound together by a metal–metal bond and additionally linked by a bridging ligand, Ph$_2$PC(CO$_2$Me)C(CO$_2$Me), which is incorporated into a four-membered metallacycle containing the iron centre, and π-coordinated to the cobalt atom through the vinyl group of the metallacycle. The Co–Fe distance of 2.583(1) Å is comparable to the corresponding bond lengths in [(OC)$_3$Co{μ-MeOC(O)CC(H)CO$_2$Me}Fe(CO)$_3$] (2.593(3) Å) [10] and in **7b** (2.595(2) Å). The structural parameters associated with the metallacycle in **8a** relate closely to those of other similar complexes [7,8,11–13]. For example, the Fe(1)–P(1)–C(3) angle of 84.3(2)° in **8a** compares with 85.1(1) and 84.6(3)° for the corresponding angles in [(OC)$_3$Ru{μ-Ph$_2$PC(Ph)C(Ph)}Co(CO)$_3$] and [(OC)$_3$-Fe{μ-η^3-Ph$_2$PC(Ph)C(Ph)}Ni(η^5-C$_5$H$_5$)], respectively, while the C(3)–C(4) bond distance of 1.451(6) Å compares with the respective distances of 1.440(6) and 1.45(1) Å in these complexes [7,12a]. The structure is completed by five terminal carbonyl groups, three on iron and two on cobalt with the Co-bound PPhMe$_2$ ligand occupying a site that is axial with respect to the metal–metal bond. It is noteworthy that in the closely related Ru–Co structure, [(OC)$_3$Ru{μ-Ph$_2$PC(Ph)-C(Ph)}Co(CO)$_3$], one of the carbonyl groups bridges the metal atoms, whilst in **8a**, all the carbonyls are terminal.

The spectroscopic properties of **7**–**9** are consistent with the structures illustrated in Scheme 4 and also with the results of the X-ray diffraction studies. Each of the complexes exhibits molecular ion and fragmentation peaks corresponding to the loss of carbonyl groups in the FAB mass spectra.

The ^{31}P-NMR spectra of **7a** and **7b** each exhibit two doublet resonances (^2J(PP) 123 Hz **7a**; 69 Hz **7b**), the signal for the metallacyclic PPh$_2$ group being located at δ −80.1 for **7a** and δ −87.9 for **7b** while the signals for the terminal phosphorus ligands are seen at δ −132.9 for the PPhMe$_2$ group (**7a**) and at δ 16.9 for the P(OMe)$_3$ group (**7b**). In both cases, the sharpness of both resonances and the large coupling constants are consistent with both phosphorus atoms being bound to iron (not Co).

In contrast to complexes **7a** and **7b**, both **8a** and **9a** have cobalt-bound phosphines. This has been deduced

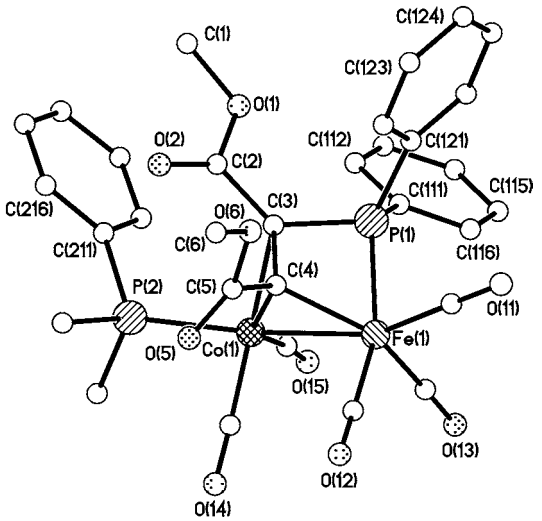

Fig. 2. Molecular structure of $[(OC)_3Fe\{\mu\text{-}PPh_2C(CO_2Me)C(CO_2Me)\}Co(CO)_2(PPhMe_2)]$ (**8a**) including the atom numbering scheme.

Table 3
Selected bond lengths (Å) and angles (°) for complex $[(OC)_3Fe\{\mu\text{-}PPh_2C(CO_2Me)C(CO_2Me)\}Co(CO)_2(PPhMe_2)]$ (**8a**)

Bond lengths			
Co(1)–Fe(1)	2.583(1)	C(1)–O(1)	1.448(6)
Co(1)–C(14)	1.772(5)	C(2)–O(2)	1.203(5)
Co(1)–C(15)	1.815(6)	C(2)–O(1)	1.354(5)
Co(1)–C(4)	1.931(5)	C(2)–C(3)	1.474(6)
Co(1)–C(3)	2.065(4)	C(3)–C(4)	1.451(6)
Co(1)–P(2)	2.226(2)	C(5)–O(5)	1.203(6)
C(4)–C(5)	1.485(7)	C(5)–O(6)	1.354(6)
Fe(1)–C(11)	1.785(6)	C(6)–O(6)	1.451(6)
Fe(1)–C(13)	1.806(6)	C(11)–O(11)	1.152(6)
Fe(1)–C(12)	1.810(6)	C(12)–O(12)	1.133(7)
Fe(1)–C(4)	2.007(5)	C(14)–O(14)	1.134(6)
Fe(1)–C(1)	2.248(2)	C(15)–O(15)	1.141(6)
P(1)–C(3)	1.780(5)	C(13)–O(13)	1.144(6)
Bond angles			
C(14)–Co(1)–C(15)	104.3(2)	C(3)–P(1)–Fe(1)	84.3(2)
C(14)–Co(1)–C(4)	99.6(2)	C(4)–C(3)–C(2)	123.3(4)
C(15)–Co(1)–C(4)	141.5(2)	C(4)–C(3)–P(1)	98.3(3)
C(14)–Co(1)–C(3)	141.5(2)	C(2)–C(3)–P(1)	129.7(3)
C(15)–Co(1)–C(3)	111.5(2)	C(4)–C(3)–Co(1)	63.9(2)
C(4)–Co(1)–C(3)	42.4(2)	C(2)–C(3)–Co(1)	122.7(3)
C(14)–Co(1)–P(2)	89.3(2)	P(1)–C(3)–Co(1)	99.2(2)
C(15)–Co(1)–P(2)	97.5(2)	C(3)–C(4)–C(5)	126.6(4)
C(4)–Co(1)–P(2)	112.7(1)	C(3)–C(4)–Co(1)	73.7(3)
C(3)–Co(1)–P(2)	99.5(1)	C(5)–C(4)–Co(1)	126.9(3)
C(14)–Co(1)–Fe(1)	89.9(2)	C(3)–C(4)–Fe(1)	102.9(3)
C(15)–Co(1)–Fe(1)	99.7(2)	C(5)–C(4)–Fe(1)	126.4(3)
C(4)–Co(1)–Fe(1)	50.3(1)	Co(1)–C(4)–Fe(1)	81.9(2)
C(3)–Co(1)–Fe(1)	70.8(1)	C(11)–Fe(1)–C(4)	115.1(2)
P(2)–Co(1)–Fe(1)	162.5(1)	C(13)–Fe(1)–C(4)	141.9(2)
C(11)–Fe(1)–C(13)	101.6(2)	C(12)–Fe(1)–C(4)	90.8(2)
C(11)–Fe(1)–C(12)	91.3(2)	C(11)–Fe(1)–P(1)	90.6(2)
C(13)–Fe(1)–C(12)	98.5(3)	C(13)–Fe(1)–P(1)	100.9(2)
C(12)–Fe(1)–P(1)	159.7(2)	C(13)–Fe(1)–Co(1)	94.2(2)
C(4)–Fe(1)–P(1)	70.2(1)	C(12)–Fe(1)–Co(1)	98.4(2)
C(11)–Fe(1)–Co(1)	160.1(2)	C(4)–Fe(1)–Co(1)	47.8(1)
P(1)–Fe(1)–Co(1)	74.4(1)		

on the basis of the ^{31}P-NMR spectra. Both **8a** and **9a** have a sharp doublet resonance (^3J(PP) 15 Hz **8a**; 9 Hz **9a**) corresponding to the ferracyclic PPh_2 group while the cobalt-bound phosphines are seen as broad resonances further downfield. The small size of these coupling constants, together with the fact that the resonances for the PPh_2H and $PPhMe_2$ ligands are broad, confirms that carbonyl substitution has occurred at the quadrupolar ^{59}Co centre.

As the results demonstrate, there is clearly a difference in the behaviour of **2** and **3** towards substitution of a carbonyl group by a phosphine or phosphite ligand. In the case of **3a**, the dimethylacetylenedicarboxylate-derived alkene group is a better π-acceptor (and a poorer σ-donor) than is the PPh_2 functionality. As a result, π-back donation to the carbonyl groups on the cobalt atom is reduced and they are thus more kinetically labile than those on the iron atom. Therefore, if a dissociative mechanism prevails, the consequence is that any donor ligand will ultimately bind to the cobalt atom. Similarly, if an associative mechanism operates, in the associative step the nucleophile will tend to attack the more electron deficient centre, namely the cobalt atom.

The opposite regiochemistry is observed in the case of **2**. This can be rationalised by considering the effect of the metallacyclic carbonyl group on the alkene and PPh_2 functionalities as donor and acceptor ligands. The presence of this carbonyl group causes both the alkene functionality and the PPh_2 group to become poorer σ-donors and better π-acceptors. In order to explain the selectivity, it requires that the electron-withdrawing effect of the carbonyl group influences the PPh_2 group more than the alkene and, by a similar argument to that above, the iron bound carbonyl groups become labilised by virtue of stronger back-donation to phosphorus (as compared to back-donation from cobalt to the alkene). Similar arguments were used to explain the regioselectivity in phosphine substitutions on $[(OC)_3Fe\{\mu\text{-}MeOC(O)CC(H)(CO_2Me)\}Co(CO)_3]$ and $[(OC)_4Fe\{\mu\text{-}ROC(O)CCH_2\}Co(CO)_3]$ (R = Me, Et), in which the former underwent substitution at cobalt, whilst the latter underwent substitution at iron [10].

2.5. Thermolysis of *9a*

As part of our studies on the reactions of organo-di-transition-metal complexes with secondary phosphines [13–16], we decided to probe the thermolysis of **9a**. We have found previously that the thermolysis of secondary phosphine-substituted alkyne-bridged bimetallic complexes results in phosphido-bridged species in which a hydrogen atom (from the cleaved PR_2H group) has migrated to the coordinated alkyne to form a bridging vinyl group [13,14]. On heating **9a** at 313 K in toluene for 22 h, however, quantitative conversion to

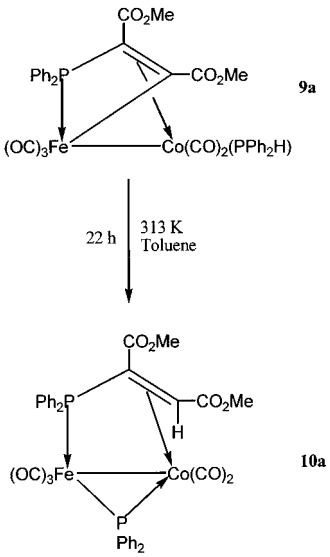

Scheme 5. The formation of complex **10a** on thermolysis of **9a**.

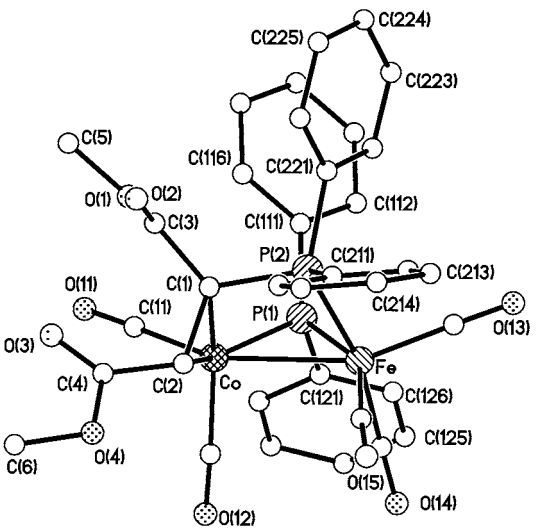

Fig. 3. Molecular structure of $[(OC)_3Fe\{\mu\text{-}PPh_2C(CO_2Me)CH(CO_2Me)\}(\mu\text{-}PPh_2)Co(CO)_2]$ (**10a**) including the atom numbering scheme.

$[(OC)_3Fe\{\mu\text{-}PPh_2C(CO_2Me)CH(CO_2Me)\}(\mu\text{-}PPh_2)Co(CO)_2]$ (**10a**) was observed (see Scheme 5). Complex **10a** was characterised by X-ray crystallography, mass spectrometry, microanalysis and by IR, ^{1}H-, ^{13}C- and ^{31}P-NMR spectroscopy (see Table 1 and Section 3).

Suitable crystals of **10a** for an X-ray diffraction study were grown by diffusion of pentane into a dichloromethane a solution of the complex at room temperature. The molecular structure of **10a** is shown in Fig. 3; selected bond lengths and angles are listed in Table 4.

The structure consists of a $Co(CO)_2$ unit bonded to an $Fe(CO)_3$ unit, and bridged by a phosphido group and a vinylphosphine ligand derived from dimethylacetylenedicarboxylate. The PPh_2 group bridges asymmetrically, with the Co–P(1) length at 2.177(2) Å being shorter than the Fe–P(1) length of 2.264(2) Å. This observation is consistent with the fact that there is stronger donation to the Co atom, which is presumably more electron deficient.

The vinylphosphine bridging ligand is coordinated through the PPh_2 functionality to iron and through the vinyl group to cobalt (i.e. in an μ:η^1(P):η^2(C) mode). In comparison with **8a**, there are several salient features. First, the Co–Fe bond in **10a** at 2.655(1) Å is significantly longer than the corresponding bond in **8a** (2.583(1) Å) possibly due to the bridging ligands in **10a** being less effective at holding the two metal centres in close proximity. In **8a**, the vinylphosphine is incorporated into a four-membered metallacycle, thus causing the bond angles within the ring to be close to 90°. For

Table 4
Selected bond lengths (Å) and angles (°) for $[(OC)_3Fe\{\mu\text{-}PPh_2C(CO_2Me)CH(CO_2Me)\}(\mu\text{-}PPh_2)Co(CO)_2]$ (**10a**)

Bond lengths			
Co–Fe	2.655(1)	Co–P(1)	2.177(2)
Co–P(2)	2.906(2)	Co–C(11)	1.763(8)
Co–C(12)	1.788(8)	Co–C(1)	2.031(6)
Co–C(2)	2.044(6)	Fe–P(1)	2.264(2)
Fe–P(2)	2.249(2)	Fe–C(13)	1.793(8)
Fe–C(14)	1.822(8)	Fe–C(15)	1.799(8)
P(2)–C(1)	1.794(6)	C(1)–C(3)	1.504(9)
O(11)–C(11)	1.147(8)	C(1)–C(2)	1.470(9)
O(13)–C(13)	1.127(8)	O(12)–C(12)	1.140(8)
O(15)–C(15)	1.140(8)	O(14)–C(14)	1.127(8)
C(2)–C(4)	1.469(9)		
Bond angles			
P(1)–Co–Fe	54.8(1)	P(2)–Co–Fe	47.4(1)
P(2)–Co–P(1)	78.4(1)	C(11)–Co–Fe	153.6(2)
C(11)–Co–P(1)	99.8(2)	C(11)–Co–P(2)	127.7(2)
C(12)–Co–Fe	94.2(2)	C(12)–Co–P(1)	99.1(2)
C(12)–Co–P(2)	135.1(2)	C(12)–Co–C(11)	97.1(3)
C(1)–Co–Fe	84.1(2)	C(1)–Co–P(1)	108.6(2)
C(1)–Co–P(2)	37.6(2)	C(1)–Co–C(11)	100.0(3)
C(1)–Co–C(12)	144.3(3)	C(2)–Co–Fe	94.0(2)
C(2)–Co–P(1)	143.2(2)	C(2)–Co–P(2)	65.2(2)
C(2)–Co–C(11)	106.6(3)	C(2)–Co–C(12)	102.6(3)
C(2)–Co–C(1)	42.3(2)	P(1)–Fe–Co	51.8(1)
P(2)–Fe–Co	72.1(1)	P(2)–Fe–P(1)	92.5(1)
C(13)–Fe–Co	155.9(2)	C(13)–Fe–P(1)	109.3(2)
C(13)–Fe–P(2)	96.7(2)	C(14)–Fe–Co	97.4(2)
C(14)–Fe–P(1)	88.2(2)	C(14)–Fe–P(2)	165.6(2)
C(14)–Fe–C(13)	96.6(3)	C(15)–Fe–Co	100.8(2)
C(15)–Fe–P(1)	150.8(3)	C(15)–Fe–P(2)	86.8(2)
C(15)–Fe–C(13)	99.7(3)	C(15)–Fe–C(14)	85.5(3)
Fe–P(1)–Co	73.4(1)	C(1)–P(2)–Co	43.7(2)
Fe–P(2)–Co	60.4(1)	C(2)–C(1)–P(2)	115.4(5)
C(1)–P(2)–Fe	102.8(2)	C(3)–C(1)–P(2)	119.5(5)
P(2)–C(1)–Co	98.7(3)	C(1)–C(2)–Co	68.4(4)
C(2)–C(1)–Co	69.3(4)	C(4)–C(2)–C(1)	117.5(6)
C(3)–C(1)–Co	125.8(5)	C(4)–C(2)–Co	117.0(5)
C(3)–C(1)–C(2)	117.4(6)		

example in **8a**, the P(1)–C(3)–C(4) angle is 98.3(3)°, and the C(3)–P(1)–Fe(1) angle is 84.3(2)°. In contrast the vinylphosphine merely bridges the two metal centres in **10a**, therefore the bond angles are larger, with P(2)–C(1)–C(2) 115.4(5)° and C(1)–P(2)–Fe at 102.8(2)°. Thirdly, the Co–vinyl carbon distances in **8a** and **10a** are noticeably different. In **10a**, the two vinyl carbon atoms appear to be equally strongly bound to the cobalt atom, with C–Co bond distances of 2.031(6) and 2.044(6) Å, whilst in **8a**, the vinyl carbon atom bound to phosphorus is significantly less strongly bound to cobalt than the other vinyl carbon atom, such that the bond distances differ by 0.13 Å (vide supra).

Apart from these differences, the bond distances between the corresponding atoms in **8a** and **10a** are closely comparable, notably the metal–carbonyl bond distances, which are all in the range 1.763(8)–1.822(8) Å in **10a** as compared with 1.772(5)–1.815(6) Å in **8a**. Also common is the fact that the two CO_2Me groups are *cis* relative to each other in both **8a** and **10a**.

The spectroscopic properties of **10a** are consistent with the solid-state structure being maintained in solution. In the ^{1}H-NMR spectrum, in addition to the phenyl and methyl protons, the vinylic proton is seen as a doublet of doublets, with coupling constants of ^3J(PH) 21.6 Hz (*trans* coupling) and ^3J(PH) 3.2 Hz (to the phosphido-bridge P atom). In the ^{31}P-NMR spectrum, there are two resonances. The downfield resonance assigned to the bridging phosphido group is broad due to bonding to the quadrupolar ^{59}Co centre and the resonance assigned to the vinylphosphine phosphorus atom is a sharp doublet with ^2J(PP) 38 Hz.

The in situ generation of a μ:η^1(P):η^2(C)–vinylphosphine ligand on a bimetallic transition-metal skeleton has previously been reported [3e,17] but, to the knowledge of the authors, its formation (in **10a**) from a μ:η^1(P):η^1(C):η^2(C)–vinylphosphine (**9a**) is unprecedented. The pathway by which **10a** is formed from **9a** is uncertain but it seems likely a hydride intermediate is involved which can subsequently undergo reductive elimination with C–H bond coupling to yield **10a**. A similar hydride intermediate has been postulated in transformation of the secondary phosphine-substituted alkyne-bridged dicobalt complex, $[Co_2\{\mu\text{-}C_2(CO_2Me)_2\}(CO)_5(PPh_2H)]$, to the phosphido-/vinyl-bridged species $[Co_2\{\mu\text{-}MeOC(O)CHC(CO_2Me)\}(\mu\text{-}PPh_2)(CO)_4]$ [14].

3. Experimental

3.1. General techniques

All reactions were carried out under a nitrogen atmosphere using standard Schlenk techniques. Solvents were distilled under nitrogen from appropriate drying agents and degassed prior to use [18]. Preparative thin-layer chromatography (TLC) was carried out on commercial Merck plates with a 0.25 mm layer of silica, or on 1 mm silica plates prepared at the University Chemical Laboratory, Cambridge. Column chromatography was performed on Kieselgel 60 (70–230 or 230–400 mesh). Products are given in order of decreasing R_f values.

The instrumentation used to obtain spectroscopic data has been described previously [19]. Unless otherwise stated, all reagents were obtained from commercial suppliers. The synthesis of $[(OC)_3Co(\mu\text{-}PPh_2)_2Co(CO)_3]$ has been reported previously [6].

3.2. Preparation of $[(OC)_4Fe(\mu\text{-}PPh_2)Co(CO)_3]$ (**1**)

To a solution of $[Co_2(\mu\text{-}PPh_2)_2(CO)_6]$ (3.07 g, 4.67 mmol) in toluene (80 cm^3) was added $[Fe(CO)_5]$ (1.83 g, 9.34 mmol) and the mixture stirred at 353 K for 0.5 h. After removal of solvent at reduced pressure, the residue was dissolved in CH_2Cl_2 and adsorbed onto silica. The silica was placed at the top of a chromatography column and eluted using hexane–dichloromethane (9:1) to give $[(OC)_4Fe(\mu\text{-}PPh_2)Co(CO)_3]$ (**1**) (1.48 g, 64%).

3.3. Reaction of $[(OC)_4Fe(\mu\text{-}PPh_2)Co(CO)_3]$ (**1**) with R^1CCR^2 ($R^1 = R^2 = CO_2Me$, Ph; $R^1 = R^2 = Ph$)

(i) To a solution of $[(OC)_4Fe(\mu\text{-}PPh_2)Co(CO)_3]$ (**1**) (0.60 g, 1.2 mmol) in THF (40 cm^3) was added dropwise $C_2(CO_2Me)_2$ (0.17 g, 1.20 mmol) and the resulting mixture stirred at 313 K for 3 h, after which all traces of starting material had disappeared. After removal of solvent under reduced pressure, the mixture was adsorbed onto silica and purified by flash column chromatography, using hexane–ethylacetate (7:3) as eluent. This yielded $[(OC)_3Fe\{\mu\text{-}PPh_2C(CO_2Me)C(CO_2Me)\}Co(CO)_3]$ (**3a**) (0.252 g, 24%) and green–brown $[(OC)_3Fe\{\mu\text{-}PPh_2C(O)C(CO_2Me)C(CO_2Me)\}Co(CO)_3]$ (**2a**) (0.210 g, 27%). Complex **2a**: (Found: C, 46.90; H, 2.55; P, 4.70. $C_{25}H_{16}CoFeO_{11}P$ requires C, 47.05; H, 2.53; P, 4.85%). FAB mass spectrum, m/z 720 [M^+] and $M^+ - nCO$ ($n = 1$–5). NMR ($CDCl_3$): ^{13}C (^{1}H composite pulse decoupled), δ 207.5[d, ^2J(PC) 25, Fe–CO], 204.6[d, ^2J(PC) 16, Fe–CO], 203.8[br, 3Co–CO], 200.3[d, ^2J(PC) 46, Fe–CO], 183.6[d, ^1J(PC) 43, $PPh_2C(O)C(CO_2Me)C(CO_2Me)$], 176.2[s, $PPh_2C(O)C(CO_2Me)C(CO_2Me)$], 167.2[d, ^3J(PC) 20, $PPh_2C(O)C(CO_2Me)C(CO_2Me)$], 136–128[m, Ph], 128.5[d, ^3J(PC) 54, $PPh_2C(O)C(CO_2Me)C(CO_2Me)$], 88.7[d, ^2J(PC) 84, $PPh_2C(O)C(CO_2Me)C(CO_2Me)$], 52.8[s, CO_2Me] and 52.7[s, CO_2Me]. Complex **3a**: (Found: C, 51.94; H, 3.85; P, 8.66. $C_{31}H_{27}CoFeO_9P_2$ requires C, 51.69; H, 3.78; P, 8.60%). FAB mass spec-

trum, m/z 720 [M^+] and $M^+ - nCO$ ($n = 1–5$). NMR ($CDCl_3$): ^{13}C (^1H composite pulse decoupled), δ 209–206[br, 3Co–CO], 202.0[s, 3Fe–CO], 174.7[d, ^3J(PC) 10, $PPh_2C(CO_2Me)C(CO_2Me)$], 167.9[s, $PPh_2C(CO_2Me)C(CO_2Me)$], 138–127[m, Ph], 132.6[d, ^2J(PC) 26, $PPh_2C(CO_2Me)C(CO_2Me)$], 53.8[d, ^1J(PC) 46, $PPh_2C(CO_2Me)C(CO_2Me)$], 52.4[s, CO_2Me] and 51.8[s, CO_2Me].

(ii) PhCCH (0.082 g, 0.81 mmol) was added dropwise to a solution of $[(OC)_4Fe(\mu\text{-}PPh_2)Co(CO)_3]$ (**1**) (0.400 g, 0.81 mmol) in THF (40 cm^3) and the mixture stirred at 318 K for 1.5 h. The solvent was then removed under reduced pressure, the residue dissolved in dichloromethane and pumped dry on silica. Elution on a chromatography column was achieved using hexane–dichloromethane (4:1), yielding traces of starting material and other unidentified products followed by brown crystalline $[(OC)_3Fe\{\mu\text{-}PPh_2C(O)CHCPh\}Co(CO)_3]$ (**2b**) (0.371 g, 77%). Complex **2b**: FAB mass spectrum, m/z 598 [M^+] and $M^+ - nCO$ ($n = 1–7$). NMR ($CDCl_3$): ^{13}C (^1H composite pulse decoupled), δ 207.1[d, ^2J(PC) 25, Fe–CO], 206.3[d, ^2J(PC) 18, Fe–CO], 205.9[br, 3Co–CO], 202.5[d, ^2J(PC) 65, Fe–CO], 186.9[d, ^1J(PC) 35, $PPh_2C(O)CHCPh$], 172.9[d, ^2J(PC) 15, $PPh_2C(O)CHCPh$], 138–127[m, Ph] and 87.5[d, ^2J(PC) 82, $PPh_2C(O)CHCPh$].

(iii) PhCCPh (0.090 g, 0.50 mmol) was added dropwise to a solution of $[(OC)_4Fe(\mu\text{-}PPh_2)Co(CO)_3]$ (**1**) (0.250 g, 0.50 mmol) in THF (30 cm^3) and stirred for 16 h at 323 K. After removal of solvent under reduced pressure, the mixture was purified by TLC using hexane–dichloromethane (4:1) as eluent to give unreacted starting material (0.107 g, 43%) and $[(OC)_3Fe\{\mu\text{-}PPh_2C(O)CPhCPh\}Co(CO)_3]$ (**2c**) (0.096 g, 29%). Complex **2c**: (Found: C, 58.91; H, 3.19; P, 4.71. $C_{33}H_{20}CoFeO_7P$ requires C, 58.78; H, 2.99; P, 4.59%). FAB mass spectrum, m/z 646 [M^+] and $M^+ - nCO$ ($n = 1–6$).

3.4. Thermolysis of $[(OC)_3Fe\{\mu\text{-}PPh_2C(O)CR^1CR^2\}Co(CO)_3]$ ($R^1 = R^2 = CO_2Me$ (**2a**), Ph (**2c**); $R^1 = H$, $R^2 = Ph$ (**2b**))

(i) A solution of $[(OC)_3Fe\{\mu\text{-}PPh_2C(O)C(CO_2Me)C(CO_2Me)\}Co(CO)_3]$ (**2a**) (0.350 g, 0.55 mmol) in THF (30 cm^3) was heated to 333 K for a period of 18 h. After removal of solvent under reduced pressure, the residue was purified by TLC, affording red crystalline $[(OC)_3Fe\{\mu\text{-}PPh_2C(CO_2Me)C(CO_2Me)\}Co(CO)_3]$ (**3a**) (0.017 g, 5%), a trace of unidentified product and decomposition products.

(ii) When a solution of $[(OC)_3Fe\{\mu\text{-}PPh_2C(O)CPhCPh\}Co(CO)_3]$ (**2c**) (0.300 g, 0.44 mmol) in THF (20 cm^3) was heated as high as 343 K over 48 h, no reaction was observed.

(iii) A solution of $[(OC)_3Fe\{\mu\text{-}PPh_2C(O)CHCPh\}Co(CO)_3]$ (**2b**) (0.400 g, 0.67 mmol) in THF (40 cm^3) was heated with stirring at 333 K for 18 h. The resulting solution was evaporated under reduced pressure and purified by TLC using hexane–ethylacetate (9:1) as eluent. This yielded orange $[(OC)_3Fe(\mu\text{-}PPh_2CPhCH)Co(CO)_3]$ (**4b**) (0.025 g, 7%), orange crystalline $[(OC)_3Fe(\mu\text{-}PPh_2CHCPh)Co(CO)_3]$ (**3b**) (0.022 g, 6%), green $[(OC)_3Fe\{\mu\text{-}PPh_2C(CHO)CPh\}Co(CO)_3]$ (**5b**) (0.011 g, 3%) and orange $[(OC)_3Fe\{\mu\text{-}PPh_2CHCPhC(O)\}Co(CO)_3]$ (**6b**) (0.041 g, 10%). Complex **4b**: FAB mass spectrum, m/z 570 [M^+] and $M^+ - nCO$ ($n = 1–5$). Complex **5b**: FAB mass spectrum, m/z 598 [M^+] and $M^+ - nCO$ ($n = 1–6$). Complex **6b**: FAB mass spectrum, m/z 598 [M^+] and $M^+ - nCO$ ($n = 1–6$). NMR ($CDCl_3$): ^{13}C (^1H composite pulse decoupled), δ 233.5[d, ^3J(PC) 12, $PPh_2CHCPhC(O)$], 210.1[d, ^2J(PC) 40, Fe–CO], 208.0[d, ^2J(PC) 15, Fe–CO], 206.4[d, ^2J(PC) 21, Fe–CO], 201.0[br, 3Co–CO], 138–127[m, Ph], 88.8[d, ^1J(PC) 25, PPh_2CHCPh] and 49.0[d, ^2J(PC) 36, PPh_2CHCPh].

3.5. Reaction of $[(OC)_3Fe\{\mu\text{-}PPh_2C(O)C(CO_2Me)C(CO_2Me)\}Co(CO)_3]$ (**2a**) with $PPhMe_2$

A solution of $PPhMe_2$ (0.043 g, 0.33 mmol) in toluene (5 cm^3) was added dropwise to a solution of $[(OC)_3Fe\{\mu\text{-}PPh_2C(O)C(CO_2Me)C(CO_2Me)\}Co(CO)_3]$ (**2a**) (0.210 g, 0.33 mmol) in toluene (25 cm^3). After stirring at 313 K for 0.5 h, the solvent was removed under reduced pressure and the residue redissolved in the minimum quantity of dichloromethane and adsorbed onto silica. The silica was added to the top of a chromatography column and eluted using hexane–ethylacetate to give deep red $[(PhMe_2P)(OC)_2Fe\{\mu\text{-}PPh_2C(O)C(CO_2Me)C(CO_2Me)\}(\mu\text{-}CO)Co(CO)_2]$ (**7a**) (0.236 g, 95%). Complex **7a**: FAB mass spectrum, m/z 748 [M^+] and $M^+ - nCO$ ($n = 1–6$).

3.6. Reaction of $[(OC)_3Fe\{\mu\text{-}PPh_2C(O)CHCPh\}Co(CO)_3]$ (**2b**) with $P(OMe)_3$

To a solution of $[(OC)_3Fe\{\mu\text{-}PPh_2C(O)CHCPh\}Co(CO)_3]$ (**2b**) (0.200 g, 0.33 mmol) was added dropwise $P(OMe)_3$ (0.041 g, 0.33 mmol). The solution was stirred for 2 h at 293 K, and the solvent stripped off under reduced pressure. The resulting residue was dissolved in the minimum amount of dichloromethane and added to the base of TLC plates and eluted with hexane–ethylacetate (7:3). This afforded purple crystalline $[\{(MeO)_3P\}(OC)_2Fe\{\mu\text{-}PPh_2C(O)CHCPh\}(\mu\text{-}CO)Co(CO)_2]$ (**7b**) (0.182 g, 78%). Complex **7b**: (Found: C, 50.13; H, 3.71; P, 8.72. $C_{29}H_{25}CoFeO_9P_2$ requires C, 50.17; H, 3.63; P, 8.92%). FAB mass spectrum, m/z 694 [M^+] and $M^+ - nCO$ ($n = 1–6$).

3.7. Reaction of $[(OC)_3Fe\{\mu\text{-}PPh_2C(CO_2Me)C(CO_2Me)\}Co(CO)_3]$ (**3a**) with PPh_2H or $PPhMe_2$

(i) To a solution of $[(OC)_3Fe\{\mu\text{-}PPh_2C(CO_2Me)C(CO_2Me)\}Co(CO)_3]$ (**3a**) (0.220 g, 0.36 mmol) in toluene (30 cm^3) was added dropwise $PPhMe_2$ (0.050 g, 0.36 mmol), and the resulting mixture stirred at 313 K. After stirring for 23 h, the solvent was removed under reduced pressure, and the residue applied to TLC plates. Elution with hexane–ethylacetate (7:3) as eluent gave red crystalline $[(OC)_3Fe\{\mu\text{-}PPh_2C(CO_2Me)C(CO_2Me)\}Co(CO)_2(PPhMe_2)]$ (**8a**) (0.218 g, 84%). Complex **8a**: (Found: C, 51.94; H, 3.85; P, 8.66. $C_{31}H_{27}CoFeO_9P_2$ requires C, 51.69; H, 3.78; P, 8.60%). FAB mass spectrum, m/z 720 [M^+] and $M^+ - nCO$ ($n = 1$–5). NMR ($CDCl_3$): ^{13}C (^1H composite pulse decoupled), δ 211.2[s, Fe–CO], 204.6[br, Co–CO], 176.3[d, ^3J(PC) 9, $PPh_2C(CO_2Me)C(CO_2Me)$], 167.5[d, ^2J(PC) 9, $PPh_2C(CO_2Me)C(CO_2Me)$], 138–127[m, Ph], 51.9[s, CO_2Me], 51.4[d, ^1J(PC) 38, $PPh_2C(CO_2Me)C(CO_2Me)$], 50.5[s, CO_2Me], 20.1[d, ^1J(PC) 31, $PPhMe_2$] and 15.1[d, ^1J(PC) 27, $PPhMe_2$].

(ii) Complex $[(OC)_3Fe\{\mu\text{-}PPh_2C(CO_2Me)C(CO_2Me)\}Co(CO)_3]$ (**3a**) (0.200 g, 0.33 mmol) in toluene (30 cm^3) and PPh_2H (0.06 g, 0.33 mmol) were used in an analogous procedure to that described in (i). Purification using TLC with hexane–ethylacetate (7:3) as eluent yielded red $[(OC)_3Fe\{\mu\text{-}PPh_2C(CO_2Me)C(CO_2Me)\}Co(CO)_2(PPh_2H)]$ (**9a**) (0.200 g, 79%). Complex **9a**: (Found: C, 54.33; H, 3.62; P, 7.83. $C_{35}H_{27}CoFeO_9P_2$ requires C, 54.71; H, 3.54; P, 8.06%). FAB mass spectrum, m/z 768 [M^+] and $M^+ - nCO$ ($n = 1$–5). NMR ($CDCl_3$): ^{13}C (^1H composite pulse decoupled), δ 210.2[s, 3Fe–CO], 204.5[br, 2Co–CO], 175.8[d, ^3J(PC) 9, $PPh_2C(CO_2Me)C(CO_2Me)$], 167.3[d, ^2J(PC) 5, $PPh_2C(CO_2Me)C(CO_2Me)$], 137–128[m, Ph], 107.5[d, ^2J(PC) 47, $PPh_2C(CO_2Me)C(CO_2Me)$], 57.8[s, CO_2Me], 50.4[s, CO_2Me] and 50.3[d, ^1J(PC) 43, $PPh_2C(CO_2Me)C(CO_2Me)$].

3.8. Thermolysis of $[(OC)_3Fe\{\mu\text{-}PPh_2C(CO_2Me)C(CO_2Me)\}Co(CO)_2(PPh_2H)]$ (**9a**)

A solution of $[(OC)_3Fe\{\mu\text{-}PPh_2C(CO_2Me)C(CO_2Me)\}Co(CO)_2(PPh_2H)]$ (**9a**) (0.140 g, 0.18 mmol) in toluene (25 cm^3) was stirred at 343 K for 22 h. After removal of the solvent under reduced pressure, the residue was applied to the base of TLC plates and eluted with hexane–ethylacetate (7:3). This yields red crystalline $[(OC)_3Fe\{\mu\text{-}PPh_2C(CO_2Me)CH(CO_2Me)\}(\mu\text{-}PPh_2)Co(CO)_2]$ (**10a**) (0.105 g, 75%). Complex **10a**: (Found: C, 54.24; H, 3.53; P, 7.86. $C_{35}H_{27}CoFeO_9P_2$ requires C, 54.71; H, 3.54; P, 8.06%). FAB mass spectrum, m/z 768 [M^+] and $M^+ - nCO$ ($n = 1$–5). NMR ($CDCl_3$): ^{13}C (^1H composite pulse decoupled), δ 211.2[s, 2Fe–CO], 174.8[d, ^3J(PC) 14, $PPh_2C(CO_2Me)CH$-

Table 5
Crystal data and structure refinement for complexes **7b**, **8a** and **10a**

	7b	**8a**	**10a**
Empirical formula	$C_{29}H_{25}CoFeO_9P_2$	$C_{31}H_{25}CoFeO_9P_2$	$C_{35}H_{27}CoFeO_9P_2$
Formula weight	693.94	720.25	768.31
Crystal system	Monoclinic	Triclinic	Tetragonal
Space group	$P2_1/n$ (alt. no. 14)	$P\bar{1}$ (no. 2)	$I4_1/a$ (no. 88)
Unit cell dimensions			
A (Å)	19.433(5)	9.412(2)	20.202(4)
b (Å)	15.329(3)	12.241(2)	–
c (Å)	10.311(2)	14.309(3)	33.379(6)
α (°)	–	83.69(3)	–
β (°)	95.28(2)	78.87(3)	–
γ (°)	–	79.61(3)	–
Z	4	2	16
μ(Mo–K_α) (mm^{-1})	0.922	1.130	0.828
Colour, habit	Purple prism	Red prism	Red prism
Crystal size/mm	$0.47 \times 0.39 \times 0.25$	$0.31 \times 0.25 \times 0.24$	$0.48 \times 0.45 \times 0.38$
θ Range (°)	3.00–25.00	3.59–25.00	3.00–25.00
Limiting hkl indices	−21 to 21, 0 to 17, 0 to 9	−10 to 11, −14 to 14, −15 to 17	−16 to 16, 0 to 24, 0 to 38
Reflections collected	4889	6954	5983
Independent reflections	1748 [$I > 3\sigma(I)$]	5570 ($R_{int} = 0.0546$)	3296 [$I > 3\sigma(I)$]
Data/restraints/parameters	1748/0/228	5552/0/397	3296/0/210
Final R indices [a]			
$I > 2\sigma(I)$	$R = 0.0558$, $R' = 0.0521$ [b]	$R_1 = 0.0480$, $wR_2 = 0.1196$	$R = 0.0559$, $R' = 0.0544$ [b]
All data		$R_1 = 0.0759$, $wR_2 = 0.1401$	

[a] $R_1 = \Sigma||F_o|-|F_c||/\Sigma|F_o|$, $wR_2 = \Sigma[w(F_o^2-F_c^2)^2]/\Sigma[w(F_o^2)^2]^2$, $w^{-1} = [\sigma^2(F_o)^2 + (aP)^2 + bP]$ with $a = 0.0512$ and $b = 2.8561$ for **8a**, $P = [\max(F_o^2,0) + 2(F_c^2)]/3$.

[b] Weights of $1/\sigma^2(F)$ were applied; $[I/\sigma(I) > 3]$ $R = \Sigma(\Delta F)/\Sigma(F_o)$; $R' = [\Sigma(\Delta F)^2/\Sigma w(F_o)^2]^2$.

(CO_2Me)], 170.9[s, $PPh_2C(CO_2Me)CH(CO_2Me)$], 143–127[m, Ph], 52.8[s, CO_2Me], 52.0[s, CO_2Me], 43.4[s, $PPh_2C(CO_2Me)CH(CO_2Me)$] and 39.0[d, ^1J(PC) 22, $PPh_2C(CO_2Me)CH(CO_2Me)$].

3.9. Crystal-structure determinations of complexes *7b*, *8a* and *10a*

X-ray intensity data were collected with graphite-monochromated Mo–K_α radiation ($\lambda = 0.71073$ Å) radiation, on a Stöe–Siemens AED four-circle diffractometer at 153(2) K for **8a** and on a Philips PW1100 four-circle diffractometer at 293(2) K for **7b** and **10a**. Details of data collection, refinement and crystal data are listed in Table 5. Lorentz-polarisation and absorption corrections were applied to the data of all the compounds. For compounds **7b** and **10a**, the positions of the metal atoms were deduced from Patterson syntheses and for **8a** the positions of most of the non-hydrogen atoms were located by direct methods. The remaining non-hydrogen atoms were revealed from subsequent difference-Fourier syntheses. For **7b** and **10a** refinement was based on F [20a], and for **8a** refinement was based on F^2 [20b]. All hydrogen atoms were placed in calculated positions with displacement parameters fixed at a value of 0.1 Å^2 in **7b** and **10a**, and set equal to $1.5U_{eq}$ of the parent carbon atoms in the structure of **8a**. Semi-empirical absorption corrections [20b] using Ψ-scans were applied to the data of **8a**, and after initial refinement with isotropic displacement parameters empirical absorption corrections [21] were applied to the data of **7b** and **10a**. All full-occupancy non-hydrogen atoms were assigned anisotropic displacement parameters in the final cycles of full-matrix least-squares refinement, apart from the carbon atoms of **10a** and the phenyl and carbonyl carbon atoms of **7b**.

4. Supplementary material

Crystallographic data for the structural analysis have been deposited with the Cambridge Crystallographic Data Centre, CCDC nos. 138793–138794. Copies of this information may be obtained free of charge from: The Director, CCDC, 12 Union Road, Cambridge, CB2 1EZ, UK (Fax: +44-1223-336033; e-mail: deposit@ccdc.cam.ac.uk or www: http://www.ccdc.cam.ac.uk).

Acknowledgements

This work was supported by the EPSRC (grant to C.-Y.M.).

References

[1] A.J. Carty, Adv. Chem. Ser. 196 (1982) 163; Pure Appl. Chem. 54 (1982)113.
[2] See for example, (a) W.F. Smith, N.J. Taylor, A.J. Carty, J. Chem. Soc. Chem. Commun. (1976) 896. (b) Y.F. Yu, J. Gallucci, A. Wojcicki, J. Chem. Soc. Chem. Commun. (1984) 653. (c) A.J. Edwards, A. Martín, M.J. Mays, D. Nazar, P.R. Raithby, G.A. Solan, J. Chem. Soc. Dalton Trans. (1993) 355. (d) N. Choi, G. Conole, M. Kessler, J.D. King, M.J. Mays, M. McPartlin, G.E. Pateman, G.A. Solan, J. Chem. Soc. Dalton Trans. (1999) 3941. (e) A.J. Carty, G. Hogarth, G.D. Enright, J.W. Steed, D. Georganopoulou, Chem. Commun. (Cambridge) (1999) 499.
[3] See for example, (a) A.J.M. Caffyn, M.J. Mays, G.A. Solan, D. Braga, P. Sabatino, A. Tiripicchio, M. Tiripicchio-Camellini, Organometallics 12 (1993) 1876. (b) R. Zolk, H. Werner, J. Organomet. Chem. 252 (1983) C53. (c) H. Werner, R. Zolk, Organometallics 4 (1985) 601. (d) A.J.M. Caffyn, M.J. Mays, G.A. Solan, G. Conole, A. Tiripicchio, J. Chem. Soc. Dalton Trans. (1993) 2345. (e) H. Werner, R. Zolk, Chem. Ber. 120 (1987) 1003. (f) H. Werner, R. Zolk, J. Organomet. Chem. 331 (1987) 95. (g) A. Martín, M.J. Mays, P.R. Raithby, G.A. Solan, J. Chem. Soc. Dalton Trans. (1993) 1789. (h) A.J. Edwards, M.J. Mays, P.R. Raithby, G.A. Solan, Organometallics 15 (1996) 4085. (i) A.J. Edwards, A. Martín, M.J. Mays, P.R. Raithby, G.A. Solan, J. Chem. Soc. Chem. Commun. (1992) 1416.
[4] B.C. Benson, R. Jackson, K.K. Joshi, D.T. Thompson, J. Chem. Soc. Chem. Commun. (1968) 1506.
[5] J.C. Burt, R. Boese, G. Schmid, J. Chem. Soc. Dalton Trans. (1978) 1387.
[6] A.D. Harley, G.J. Guskey, G.L. Geoffroy, Organometallics 2 (1983) 53.
[7] (a) R. Regragui, P.H. Dixneuf, N.J. Taylor, A.J. Carty, Organometallics 9 (1990) 2234. (b) R. Regragui, P.H. Dixneuf, N.J. Taylor, A.J. Carty, Organometallics 3 (1984) 814.
[8] S.L. Ingham, M.J. Mays, P.R. Raithby, G.A. Solan, B.V. Sundavadra, G. Conole, M. Kessler, J. Chem. Soc. Dalton Trans. (1994) 3607.
[9] A.J.M. Caffyn, M.J. Mays, G.A. Solan, D. Braga, P. Sabatino, G. Conole, M. McPartlin, H.R. Powell, J. Chem. Soc. Dalton Trans. (1991) 3103.
[10] (a) I. Moldes, J. Ros, R. Mathieu, X. Solans, M. Fontbardia, J. Chem. Soc. Dalton Trans. (1987) 1619. (b) I. Moldes, J. Ros, R. Mathieu, X. Solans, M. Fontbardia, J. Organomet. Chem. 423 (1992) 65.
[11] J.D. King, M.J. Mays, G.E. Pateman, P.R. Raithby, M.A. Rennie, G.A. Solan, N. Choi, G. Conole, M. McPartlin, J. Chem. Soc. Dalton Trans. (1999) 4447.
[12] (a) H. Yamazaki, K. Aoki, H. Yamazaki, J. Organomet. Chem. 84 (1975) C28. (b) B.L. Barnett, C. Kruger, Cryst. Struct. Comm. 2 (1973) 347. (c) B. Klingert, A.L. Rheingold, H. Werner, Inorg. Chem. 27 (1988) 1354. (d) F. Van Gastel, A.J. Carty, M.A. Pellinghelli, A. Tiripicchio, E. Sappa, J. Organomet. Chem. 385 (1990) C50. (e) G. Conole, K.A. Hill, M. McPartlin, M.J. Mays, M.J. Morris, J. Chem. Soc. Chem. Commun. (1989) 688. (f) M.J. Mays, P.F. Reinisch, G.A. Solan, M. McPartlin, H.R. Powell, J. Chem. Soc. Dalton Trans. (1995) 1597.
[13] A. Martín, M.J. Mays, P.R. Raithby, G.A. Solan, J. Chem. Soc. Dalton Trans. (1993) 1431.
[14] A.J.M. Caffyn, M.J. Mays, G. Conole, M. McPartlin, H.R. Powell, J. Organomet. Chem. 436 (1992) 83.
[15] M.J. Mays, G.E. Pateman, G.A. Solan, unpublished results.
[16] A.J.M. Caffyn, A. Martín, M.J. Mays, P.R. Raithby, G.A. Solan, J. Chem. Soc. Dalton Trans. (1994) 609.
[17] (a) R.S. Dickson, O.M. Paravagna, Organometallics 11 (1992) 3196. (b) K. Henrick, M. McPartlin, J.A. Iggo, A. Kemball, M.J. Mays, P.R. Raithby, J. Chem. Soc. Dalton Trans. (1987) 2669.

(c) G. Conole, M. McPartlin, M.J. Mays, M.J. Morris, J. Chem. Soc. Dalton Trans. (1990) 2359.
[18] W.L.F. Armarego, D.D. Perrin, Purification of Laboratory Chemicals, fourth ed., Butterworth Heinemann, London, 1996.
[19] A.J.M. Caffyn, M.J. Mays, P.R. Raithby, J. Chem. Soc. Dalton Trans. (1991) 2349.
[20] (a) G.M. Sheldrick, SHELX-76, Program for Crystal Structure Determination, University of Cambridge, 1976. (b) SHELXTL (PC version 5.03), Siemens Analytical Instruments Inc., Madison, WI, 1994.
[21] N. Walker, D. Stuart, Acta Crystallogr. Sect. A 39 (1983) 158.